International Journal of Fracture **85:** 111–130, 1997.

Approximate methods for predicting J-integral of a circumferentially surface-cracked pipe subject to bending

S. RAHMAN[1] and F.W. BRUST[2]
[1]*Department of Mechanical Engineering, The University of Iowa, Iowa City, IA 52242*
[2]*Engineering Mechanics Group, Battelle, 505 King Avenue, Columbus, OH 43201*
e-mail: rahman@icaen.uiowa.edu, website: http://www.icaen.uiowa.edu/∼rahman

Received 10 September 1996; accepted in revised form 7 May 1997

Abstract. This study proposes two new methods to estimate the energy release rate of a circumferentially cracked pipe with an internal, constant-depth, finite-length surface flaw subjected to pure bending loads. The methods are based on the deformation theory of plasticity, constitutive law characterized by Ramberg–Osgood model, and an equivalence criterion incorporating reduced thickness analogy for simulating system compliance due to the presence of a crack. Closed-form solutions were developed in terms of elementary functions for an approximate evaluation of J-integral. They are general and can be applied in the complete range between elastic and fully plastic conditions. Several numerical examples are presented to illustrate the proposed methods. The comparisons with the results of elastic–plastic finite element analysis showed satisfactory prediction of J-integral by one of the proposed methods.

Key words: elastic–plastic fracture mechanics, J-integral, surface crack, pipe, finite element method, energy release rate.

1. Introduction

Aside from ideally brittle materials, any loading of a cracked engineering structure is accompanied by inelastic deformation in the neighborhood of the crack tip due to stress concentration. Consequently, the ultimate utility of linear-elastic fracture mechanics (LEFM) must necessarily depend on the extent of inelastic deformation being small compared with the size of the crack and any other characteristic length. For materials with high toughness and low strength, it is virtually impossible to satisfy this condition due to extensive plastic deformation around a crack tip. Cracked components made of these materials, which pose serious threat to structural integrity, are reactor pressure vessels, steam generator vessels, pressurizer vessels, piping, and steam generator tubes of a modern nuclear power plant. In much or all of the working temperature regime of these structural components, the material is being typically stressed above the brittle-to-ductile transition temperature where the fracture response is essentially ductile and the material is capable of considerable inelastic deformation. These issues are not unique to the nuclear industry. Identical conditions also prevail in others, notably in chemical and fossil plants and aerospace and aircraft propulsion. As such, theories based on elastic–plastic fracture mechanics (EPFM) are needed to obtain realistic measures of fracture behavior of cracked structural systems.

Recent analytical and experimental studies on EPFM indicate that the energy release rate (also known as the J-integral) and crack-tip opening displacement (CTOD) are the most viable fracture parameters for characterizing initiation of crack growth, stable crack growth, and subsequent instability in ductile materials (Rice, 1968; Hutchinson, 1982). This clearly suggests that the fracture parameters like J and/or CTOD can be conveniently used to assess structural integrity for both leak-before-break and in-service flaw acceptance criteria in degraded piping systems. It is, however, noted that the parameter J still possesses some theoretical limitations. For example, the Hutchinson–Rice–Rosengren (HRR) singular field (Rice and Rosengren, 1968; Hutchinson, 1968) may not be valid in the case of certain amount of crack extension where J ceases to act as amplifier for this singular field. Nevertheless, possible error is considered tolerable if the relative amount of crack extension stays within a certain limit and if elastic unloading and non-proportional plastic loading zones around a crack tip are surrounded by a much larger zone of nearly proportional loading controlled by the HRR field. Under this condition of J-dominance, both the onset and limited amount of crack growth can be correlated to the critical values of J and J-resistance curve, respectively (Paris et al., 1979).

The evaluation of energy release rates in circumferentially cracked pipes is usually performed by (1) numerical analysis and (2) estimation techniques. Traditionally, a comprehensive numerical study has been based on elastic–plastic finite element method (FEM) for nonlinear stress analysis. In general, the FEM provides accurate results for the fracture response, but it can be expensive and time-consuming to be used routinely. On the other hand, simple mathematical models, often referred to as J-estimation models, can also be used or developed to predict J or other fracture parameters of interest from elastic–plastic fracture theories. However, these models often require simpler representations of the material's stress-strain behavior, flaw shape, orientation, loading, and boundary conditions. If these assumptions are acceptable, then the J-estimation method provides an alternative means for characterizing fracture response with much less computational cost when compared with the FEM. Due to approximations, however, the J-estimation methods, in general, are less accurate than the FEM and hence, often requires validation with the latter method.

For circumferentially surface-cracked pipes, perhaps the GE/EPRI method (Kumar and German, 1988) is the first J-estimation method developed to predict J-integral and other fracture parameters. In this method, Kumar and German (1988) compiled a series of FEM solutions for several crack sizes, pipe geometries, and material properties in a handbook form. For example, dimensionless influence functions were developed using the line-spring finite-element results for predicting J, the crack-opening displacement, and pipe rotations. For any arbitrary new problem, the solution is usually achieved from multiple interpolation (and extrapolation, if necessary) of the tabulated results. For surface-cracked pipe, the only functions developed initially were those for 360-degree circumferential cracks under pure tensile loading. For pure bending loads, the functions for finite-length cracks were subsequently determined for a very limited number of cases. The primary limitation of this method involves the errors introduced in the interpolation and extrapolation of limited tabulated influence functions. In addition, no such functions were developed for deep surface-cracked pipes. Realizing these limitations, Ahmad et al. (1989) developed an estimation scheme to predict J and moment-rotation behavior under pure bending using the existing GE/EPRI functions for 360-degree surface cracks under tensile loading. Tables of various dimensionless functions required for the numerical calculations were developed by Ahmad et al. (1989) and incorporated into two resulting computer codes, known as the SC.TNP and SC.TKP, for analyzing thin-walled and thick-walled pipes, respectively (Scott and Ahmad, 1987). There are three limitations in this method. First, this method involves a 'disposable' length parameter which represents the distance from the plane of the crack to that cross-section where the stresses are assumed to be uniform. This parameter is not well-defined and the results vary significantly with the choice of this parameter. Second, the GE/EPRI functions for deeply cracked specimens are not available. Third, the method is applicable only for pure bending loads. Combined loads cannot be handled by this method. However, it must be noted that this was the only J-estimation scheme available for finite-length surface-cracked pipes under pure bending loads. To evaluate the accuracy of SC.TNP and SC.TKP methods, Krishnaswamy et al. (1995) conducted a computational study by comparing the predicted J-integral solutions with those from elastic–plastic finite element analysis. The results showed that further refinements are necessary to improve the predictions of SC.TNP and SC.TKP methods. In consequence, two research directions were pursued. One study involved refinement of SC.TNP and SC.TKP methods by modifying the length parameter so that it becomes an empirical function of wall thickness and material hardening constant (Krishnaswamy et al., 1995). The other study involved development of a new J-estimation method without having to depend on the GE/EPRI influence functions. This paper presents the analytical developments and findings of the latter study.

In this study, two new methods were developed to predict the energy release rate of a circumferentially cracked pipe with an internal, constant-depth, finite-length surface flaw subjected to pure bending loads. The methods are based on (1) the deformation theory of plasticity, (2) constitutive law characterized by Ramberg–Osgood power-law model, and (3) an equivalence criterion incorporating reduced thickness analogy for simulating system compliance due to the presence of a crack. Closed-form solutions were developed in terms of elementary functions for an approximate evaluation of J-integral. The methods are general in the sense that they may be applied in the complete range between elastic and fully plastic conditions. Since they are based on J-tearing theory, they are subject to the usual limitations imposed upon this theory, e.g., proportional loading, etc. This has the implication that the crack growth must be small, although in practice, J-tearing methodology is used far beyond the limits of its theoretical validity with acceptable results (Wilkowski et al., 1989; Schmidt et al., 1991; Wilkowski et al., 1991–1994; Hopper et al., 1995). Several numerical examples are presented to illustrate the proposed methods which were verified with the reference solutions from elastic–plastic finite element analysis.

2. General background

The J-estimation methods developed in this study can be best described with the aid of Figure 1. As shown in Figure 1(a), a circumferential constant-depth, internal, surface crack is assumed to exist in the pipe that has mean radius, R_m, and wall thickness, t. The depth and total angle of the surface crack are denoted by a and 2θ, respectively. The crack is symmetrically placed with respect to the bending plane of the pipe. The crack is located sufficiently far from the pipe ends such that the end effects on crack-driving force are inconsequential. In Figure 1(b), the pipe is subjected to a pure bending moment, M, applied at the remote ends and the resulting rotation of one pipe end relative to the other end is denoted by ϕ. In the development of a J-estimation scheme, it is generally assumed that the load-point rotation due to the presence of crack, ϕ^c, and the crack driving force, J, can be split into elastic and plastic components

$$\phi^c = \phi_e^c + \phi_p^c, \tag{1}$$

$$J = J_e + J_p, \tag{2}$$

where the subscripts 'e' and 'p' refer to elastic and plastic contributions, respectively. In the elastic range, ϕ_e^c and M are uniquely related. In addition, if the deformation theory of

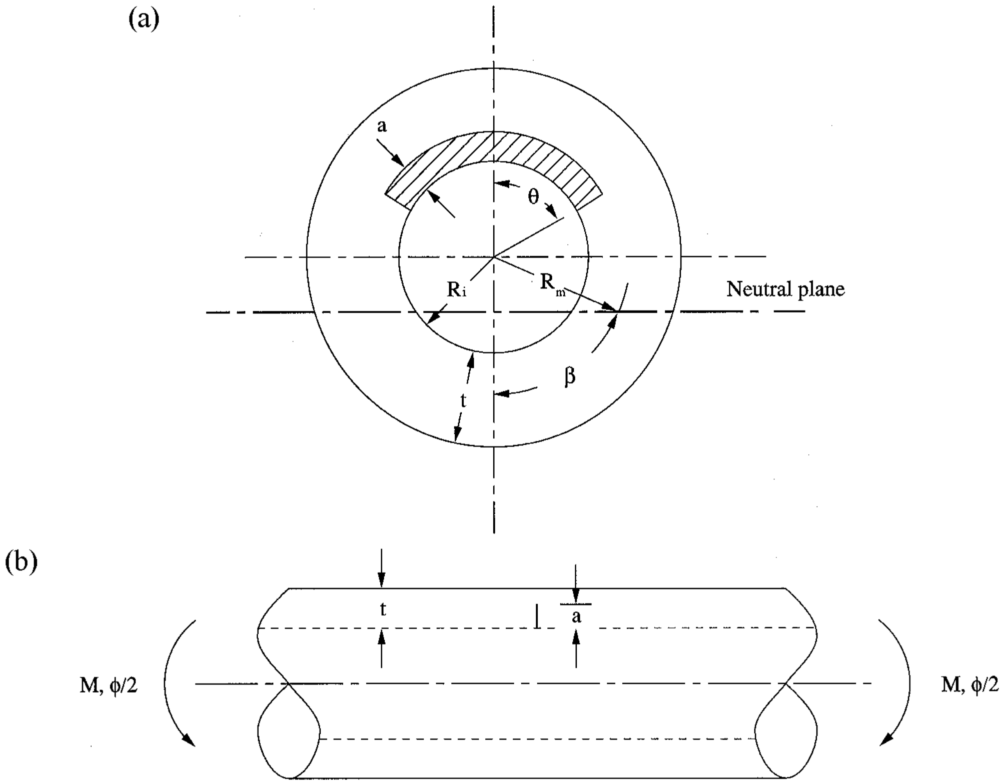

Figure 1. Schematic of idealized surface-cracked pipe geometry and loading (a) Pipe cross-section containing a surface crack, (b) Surface-cracked pipe under pure bending.

plasticity holds, a unique relationship also exists between ϕ_p^c and M. Once these relationships are determined, the elastic component, J_e, and the plastic component, J_p, of the total energy release rate, J, can be obtained readily.

3. The elastic solution

The elastic energy release rate, J_e, at the point of maximum depth can be defined as

$$J_e = \frac{\partial U^T}{\partial A} = \frac{\partial}{\partial A}(U^c + U^{nc}) = \frac{\partial U^c}{\partial A}, \tag{3}$$

where U^T is the total internal strain energy, U^{nc} is the strain energy which would exist if there were no crack present, $U^c = U^T - U^{nc}$ is the additional strain energy in the pipe due to the presence of a crack, and $A = 2a\theta(R_m - t/2 + a/2)$ is the cracked area. For thin-walled pipe with mode-I crack growth, J_e at the point of maximum depth can be obtained as

$$J_e = \frac{K_{\mathrm{I}}^2}{E'}, \tag{4}$$

where $E' = E/(1-\nu^2)$ for plane strain condition with E and ν representing elastic modulus and Poisson's ratio of the material, respectively, and K_{I} is the mode-I stress intensity factor. From the LEFM theory, K_{I} at the deepest point of the crack is given by

$$K_{\mathrm{I}} = \frac{M}{\pi R_m^2 t} F_B(a/t, \theta/\pi)\sqrt{\pi a}, \tag{5}$$

in which $F_B(a/t, \theta/\pi)$ is a geometry function relating K_{I} of a cracked pipe to that for the same size (depth) of a through-wall crack in an infinite plate. In general, F_B should be a function of $a/t, \theta/\pi$, and R_m/t. But, according to Article IWB-3650 in Section XI of the ASME Code[1] (1992),

$$F_B(a/t, \theta/\pi) = 1.1 + \frac{a}{t}\left[-0.09967 + 5.0057\left(\frac{a}{t}\frac{\theta}{\pi}\right)^{0.565} - 2.8329\left(\frac{a}{t}\frac{\theta}{\pi}\right)\right]. \tag{6}$$

Clearly, F_B represented by Equation 6 does not have an explicit functional dependency on the R_m/t ratio of the pipe. Preliminary results from authors' linear-elastic finite element analysis suggest that this equation may not be satisfactory for $R_m/t \geqslant 20$. Work is currently underway at the University of Iowa and Battelle to critically evaluate the adequacy of Equation 6 and develop new expressions for $F_B(a/t, \theta/\pi)$, if necessary. Nevertheless, Equation 6 was used in the present study, because it was the only equation available at that time for representing F_B of constant-depth surface flaws in pipes. From Equations 3 to 5, U^c can be integrated to yield

$$U^c = \frac{M^2}{\pi R_m^4 t^2 E'}\,\mathrm{I}_B(a/t, \theta/\pi), \tag{7}$$

where

$$\mathrm{I}_B(a/t, \theta/\pi) = 2\theta(R_m - \tfrac{1}{2}t)\int aF_B^2(a/t, \theta/\pi)da + 2\theta\int a^2F_B^2(a/t, \theta/\pi)\,\mathrm{d}a. \tag{8}$$

Using Castigliano's Theorem

$$\phi_e^c = \frac{\partial U^c}{\partial M}, \tag{9}$$

which when combined with Equation 7 gives

$$\phi_e^c = \frac{2M}{\pi R_m^4 t^2 E'}\,\mathrm{I}_B(a/t, \theta/\pi), \tag{10}$$

as a relationship between moment and elastic rotation. Equations 4 through 6 completely specify the elastic energy release rate, J_e, and hence the elastic solution is complete in closed form. The integral in Equation 8 can be evaluated using the expression of $F_B(a/t, \theta/\pi)$ given by Equation 6. Explicit functional form of $\mathrm{I}_B(a/t, \theta/\pi)$ is given in Appendix A.

[1] F_B in Equation 6 was originally developed in 1989–1991 by Novetech Corporation for Electric Power Research Institute during the compilation of Ductile Fracture Handbook (Volume 2). Equation 6 has been claimed to be valid for $0.08 \leqslant a/t \leqslant 0.8$, $0.05 \leqslant \theta/\pi \leqslant 0.5$, and $5 \leqslant R_m/t \leqslant 10$.

4. The plastic solution

The plastic energy release rate, J_p, also at the point of maximum depth, can be defined as

$$J_p = \int_0^M \frac{\partial \phi_p^c}{\partial A}\,\mathrm{d}M = \frac{\partial}{\partial A}\int_0^M \phi_p^c\,\mathrm{d}M, \tag{11}$$

the evaluation of which requires determination of $M - \phi_p^c$ relationship. When this relationship is obtained, Equation 11 can be used to find J_p and can then be added to J_e to determine the total J according to Equation 2.

A widely used univariate constitutive law describing material's stress-strain ($\sigma - \varepsilon$) relation is the well-known Ramberg–Osgood model given by

$$\frac{\varepsilon}{\varepsilon_0} = \frac{\sigma}{\sigma_0} + \alpha\left(\frac{\sigma}{\sigma_0}\right)^n, \tag{12}$$

where σ_0 is a reference stress, which can be arbitrary, but typically assumed to be the yield stress, $\varepsilon_0 = \sigma_0/E$ is the associated reference strain, and α and n are the parameters of above power-law model usually chosen from a best fit of experimental data. In applying the Ramberg–Osgood equation to the cracked pipe problem, it is necessary to relate the stresses (or moments) with rotations. Ilyushin showed that the field solutions to the boundary value problem involving a monotonically increasing load or displacement type parameter is ‘proportional’ (Ilyushin, 1946). Consequently, Equation 12 applies (minus the elastic term) and the deformation theory plasticity is assumed to be valid. Thus

$$\phi_p^c \propto M^n, \tag{13}$$

giving

$$\phi_p^c = \hat{C}M^n, \tag{14}$$

where $\hat{C}$ is a proportionality constant which can be determined via FEM. In this study, an alternative analytical formulation was developed to evaluate $\hat{C}$ and hence, estimate J_p.

4.1. Evaluation of $\hat{C}$

Suppose that the actual pipe can be replaced by a pipe with reduced thickness, t_e, which extends for a distance, $\hat{a}$ at the center as shown in Figure 2. Far from the crack plane, the rotation of the pipe is not greatly influenced by whether a crack exists or some other discontinuity is present as long as the discontinuity can approximate the effects of crack. The reduced thickness section, which actually results in material discontinuity, is an attempt to simulate the reduced system compliance due to the presence of crack. This equivalence approach was originally suggested by Brust (1987) for analyzing through-wall-cracked pipes with base-metal cracks under pure bending. Later Rahman and Brust successfully implemented the similar approach to evaluate J for through-wall-cracked pipes with weld-metal cracks that can account for both base- and weld-metal tensile properties (Rahman et al., 1991; Rahman and Brust, 1992; Rahman et al., 1996). It is assumed here that the deformation theory of plasticity controls stress-strain response and that the beam theory holds.

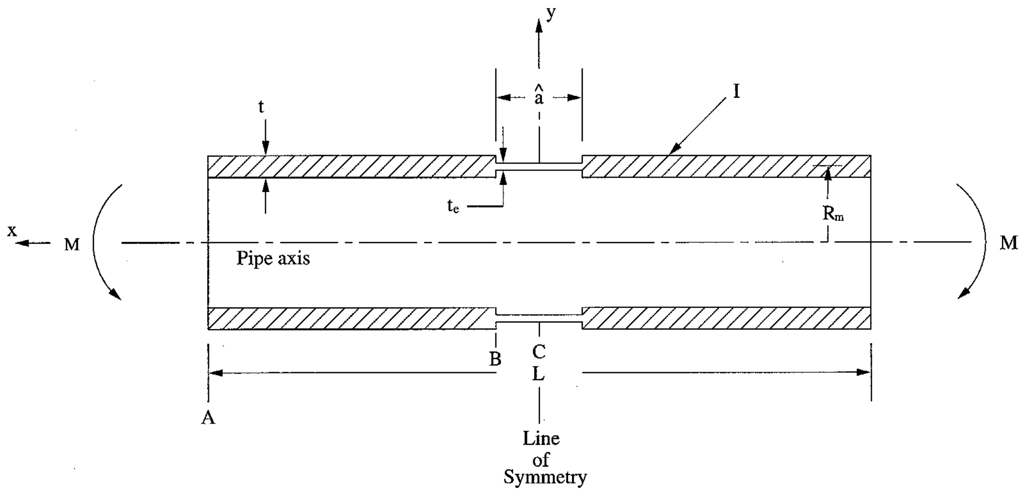

Figure 2. Reduced section analogy by the SC.ENG1 and SC.ENG2 methods.

Consider the equivalent pipe with material discontinuity in Figure 2 which is subjected to bending load, M at both ends. Using classical beam theory, the ordinary differential equations governing displacement of beams with Ramberg–Osgood constitutive law (plastic part only) can be easily derived. These equations, when supplemented by the appropriate boundary and compatibility conditions, can be solved following elementary operations of calculus. Details of algebra associated with these solutions are provided in Appendix B. The rotations ($\mathrm{d}y/\mathrm{d}x$ in Equations 60 and 63 of Appendix B) provide relationship between far-field plastic rotation due to material discontinuity and the corresponding elastic rotations. According to the equivalence method, the same relationship is assumed to hold between ϕ_p^c and ϕ_e^c. In general, such a relationship would depend on geometry, material properties of pipe, equivalent thickness, t_e, and also the spatial coordinate, x (see Figure 2). In particular, when the spatial location is selected to be the point B (i.e., at $x = \hat{a}/2$), the explicit relationship between ϕ_p^c and ϕ_e^c becomes

$$\phi_p^c = \left(\frac{t}{t_e}\right)^{n-1} \left(\frac{\pi}{4\hat{K}}\right)^n \alpha \left(\frac{M}{M_0}\right)^{n-1} \phi_e^c, \tag{15}$$

in which

$$M_0 = \pi R_m^2 t \sigma_0, \tag{16}$$

$$\hat{K} = \frac{\sqrt{\pi}}{2} \frac{\Gamma\left(1 + \frac{1}{2n}\right)}{\Gamma\left(\frac{3}{2} + \frac{1}{2n}\right)}, \tag{17}$$

with

$$\Gamma(u) = \int_0^\infty \xi^{u-1} \exp(-\xi)\, \mathrm{d}\xi, \tag{18}$$

representing the gamma function. Following the substitution of ϕ_e^c from Equation 10 into Equation 15, ϕ_p^c becomes

$$\phi_p^c = \left(\frac{t}{t_e}\right)^{n-1} \left(\frac{\pi}{4\hat{K}}\right)^n \alpha \left(\frac{M}{M_0}\right)^{n-1} \frac{2M}{\pi R_m^4 t^2 E'} \, \mathrm{I}_B(a/t, \theta/\pi), \tag{19}$$

which, when compared with Equation 14, yields

$$\hat{C} = \frac{\alpha}{M_0^{n-1}} \left(\frac{\pi}{4\hat{K}} \right)^n H(a/t)^{n-1} G(a/t), \tag{20}$$

where

$$H(a/t) = \frac{t}{t_e} \tag{21}$$

and

$$G(a/t) = \frac{2}{\pi R_m^4 t^2 E'} \, \mathrm{I}_B(a/t, \theta/\pi). \tag{22}$$

Following differentiation with respect to crack depth, a, the partial derivative of $\hat{C}$ is

$$\frac{\partial \hat{C}}{\partial a} = \frac{\alpha}{t M_0^{n-1}} \left(\frac{\pi}{4\hat{K}} \right)^n \left[H(a/t)^{n-1} \frac{\mathrm{d}G(a/t)}{\mathrm{d}(a/t)} + (n-1) G(a/t) H(a/t)^{n-2} \frac{\mathrm{d}H(a/t)}{\mathrm{d}(a/t)} \right], \tag{23}$$

where

$$\frac{\mathrm{d}G(a/t)}{\mathrm{d}(a/t)} = \frac{2}{\pi R_m^4 t^2 E'} \frac{\mathrm{d}\mathrm{I}_B(a/t, \theta/\pi)}{\mathrm{d}(a/t)} \tag{24}$$

and

$$\frac{\mathrm{d}\mathrm{I}_B(a/t, \theta/\pi)}{\mathrm{d}(a/t)} = at[2\theta(R_m - t/2) + 2\theta a] F_B^2(a/t, \theta/\pi). \tag{25}$$

The explicit expressions for the functions $H(a/t)$ and $\mathrm{d}H(a/t)/\mathrm{d}(a/t)$ depend on the type of limit-load solutions for surface-cracked pipes. They are discussed in the forthcoming sections.

4.2. Estimation of J_p

Having determined $\hat{C}$ and $\partial\hat{C}/\partial a$, Equation 11 can be simplified further to evaluate J_p. Following simple algebra, it can be shown that

$$J_p = \frac{\alpha (M/M_0)^{n+1} (\pi/4\hat{K})^n}{2t\theta(R_m - t/2 + a)(n+1)} \left[H(a/t)^{n-1} \frac{\mathrm{d}G(a/t)}{\mathrm{d}(a/t)} + (n-1) G(a/t) H(a/t)^{n-2} \frac{\mathrm{d}H(a/t)}{\mathrm{d}(a/t)} \right]. \tag{26}$$

Equation 26 provides a simple closed-form solution of J_p.

5. The SC.ENG1 and SC.ENG2 methods

The evaluation of J_p in Equation 26 requires determination of $H(a/t)$ and $\mathrm{d}H(a/t)/\mathrm{d}(a/t)$. According to the definition of $H(a/t)$ (see Equation 21), this also requires estimation of equivalent thickness, t_e for the uncracked pipe. In the equivalence method proposed here t_e can be determined by forcing the net-section-collapse moment of the equivalent uncracked pipe to be equal to the net-section-collapse moment of the actual cracked pipe. For an uncracked pipe with reduced thickness, t_e, the net-section-collapse moment, M_L^d, is

$$M_L^d = 4\sigma_f R_m^2 t_e, \tag{27}$$

where σ_f is the flow or collapse stress of the material. However, in determining the net-section-collapse moment, M_L^c, for circumferential surface-cracked pipe, there are several solutions available in the current literature. In this study, two such equations, based on original and Kurihara modifications, were used to determine $H(a/t)$ and its derivative for the evaluation of J_p. Accordingly, the expressions of J_p based on $H(a/t)$ and $\mathrm{d}H(a/t)/\mathrm{d}(a/t)$ obtained from the original net-section-collapse equations (Kanninen et al., 1976) and Kurihara modification to the net-section-collapse equations (Kurihara et al., 1988) are defined as the SC.ENG1 and the SC.ENG2 methods, respectively. The explicit details for the evaluations of $H(a/t)$ and $\mathrm{d}H(a/t)/\mathrm{d}(a/t)$ by these two methods are given in the next sections.

5.1. THE SC.ENG1 METHOD

The following are the original equations for the net-section-collapse moment, M_L^c (Kanninen et al., 1976) of a surface-cracked pipe under pure bending and the resulting expressions for $H(a/t)$ and $\mathrm{d}H(a/t)/\mathrm{d}(a/t)$ used by the SC.ENG1 method. For $\beta \leqslant \pi - \theta$,

$$M_L^c = 2R_m^2 t\sigma_f \left[2\,\sin\,\beta - \frac{a}{t}\,\sin\,\theta\right], \tag{28}$$

where

$$\beta = \frac{\pi - \theta(a/t)}{2}. \tag{29}$$

When the limit loads from Equations 27 and 28 are made equal

$$H(a/t) = \frac{2}{2\,\sin\frac{\pi-\theta(a/t)}{2} - \frac{a}{t}\,\sin\,\theta} \tag{30}$$

and

$$\frac{\mathrm{d}H(a/t)}{\mathrm{d}(a/t)} = \frac{2\left[\theta\,\cos\frac{\pi-\theta(a/t)}{2} + \sin\,\theta\right]}{\left[2\,\sin\frac{\pi-\theta(a/t)}{2} - \frac{a}{t}\sin\,\theta\right]^2}. \tag{31}$$

For $\beta \geqslant \pi - \theta$

$$M_L^c = 2R_m^2 t\sigma_f \left[2 - \frac{a}{t}\right]\sin\,\beta, \tag{32}$$

where

$$\beta = \frac{\pi(1 - a/t)}{2 - a/t}. \tag{33}$$

When the limit loads from Equations 27 and 32 are made equal

$$H(a/t) = \frac{2}{(2 - a/t)\sin\frac{\pi(1-a/t)}{2-a/t}} \tag{34}$$

and

$$\frac{\mathrm{d}H(a/t)}{\mathrm{d}(a/t)} = \frac{\frac{2\pi}{2-a/t}\cos\frac{\pi(1-a/t)}{2-a/t} + 2\sin\frac{\pi(1-a/t)}{2-a/t}}{\left[(2-a/t)\sin\frac{\pi(1-a/t)}{2-a/t}\right]^2}. \tag{35}$$

5.2. The SC.ENG2 method

The following are the Kurihara modifications to the equations for the net-section-collapse moment, M_L^c (Kurihara et al., 1988) of a surface-cracked pipe under pure bending and the resulting expressions for $H(a/t)$ and $\mathrm{d}H(a/t)/\mathrm{d}(a/t)$ used by the SC.ENG2 method. For $\beta \leqslant \pi - \theta$

$$M_L^c = 2R_m^2 t\sigma_f\left[2m\sin\beta + \left(1 - \frac{a}{t} - m\right)\sin\theta\right], \tag{36}$$

where

$$\beta = \tfrac{1}{2}\pi + \frac{\theta(1 - a/t - m)}{2m}. \tag{37}$$

When the limit loads from Equations 27 and 36 are made equal

$$H(a/t) = \frac{2}{K_1(a/t)} \tag{38}$$

and

$$\frac{\mathrm{d}H(a/t)}{\mathrm{d}(a/t)} = -\frac{2}{K_1(a/t)^2}\frac{\mathrm{d}K_1(a/t)}{\mathrm{d}(a/t)}, \tag{39}$$

where

$$K_1(a/t) = 2m\sin\left[\tfrac{1}{2}\pi + \frac{\theta(1-a/t-m)}{2m}\right] + (1 - a/t - m)\sin\theta \tag{40}$$

and

$$\begin{aligned}\frac{\mathrm{d}K_1(a/t)}{\mathrm{d}(a/t)} = & -\frac{1}{m}\cos\left[\tfrac{1}{2}\pi + \frac{\theta(1-a/t-m)}{2m}\right]\left[m\theta + \theta(1-a/t)\frac{\partial m}{\partial(a/t)}\right] \\ & + \frac{2\partial m}{\partial(a/t)}\sin\left[\tfrac{1}{2}\pi + \frac{\theta(1-a/t-m)}{2m}\right] - \left[1 + \frac{\partial m}{\partial(a/t)}\right]\sin\theta.\end{aligned} \tag{41}$$

For $\beta \geqslant \pi - \theta$

$$M_L^c = 2R_m^2 t\sigma_f\left[1 - \frac{a}{t} + m\right]\sin\beta, \tag{42}$$

where

$$\beta = \frac{\pi(1 - a/t)}{1 - a/t + m}. \tag{43}$$

When the limit loads from Equations 27 and 42 are made equal

$$H(a/t) = \frac{2}{K_2(a/t)} \tag{44}$$

and

$$\frac{\mathrm{d}H(a/t)}{\mathrm{d}(a/t)} = -\frac{2}{K_2(a/t)^2}\frac{\mathrm{d}K_2(a/t)}{\mathrm{d}(a/t)}, \tag{45}$$

where

$$K_2(a/t) = Q_1(a/t)\sin Q_2(a/t), \tag{46}$$

$$\frac{\mathrm{d}K_2(a/t)}{\mathrm{d}(a/t)} = Q_1 \cos Q_2\frac{\mathrm{d}Q_2}{\mathrm{d}(a/t)} + \sin Q_2\frac{\mathrm{d}Q_1}{\mathrm{d}(a/t)}, \tag{47}$$

$$Q_1(a/t) = 1 - \frac{a}{t} + m, \tag{48}$$

$$Q_2(a/t) = \frac{\pi(1 - a/t)}{Q_1(a/t)}, \tag{49}$$

$$\frac{\mathrm{d}Q_1}{\mathrm{d}(a/t)} = -1 + \frac{\partial m}{\partial(a/t)} \tag{50}$$

and

$$\frac{\mathrm{d}Q_2}{\mathrm{d}(a/t)} = -\frac{\pi Q_1 + \pi(1 - a/t)\frac{\mathrm{d}Q_1}{\mathrm{d}(a/t)}}{Q_1^2}. \tag{51}$$

In Equations 36 through 51, the functions $m(a/t, \theta/\pi)$ and $\partial m(a/t, \theta/\pi)/\partial(a/t)$ are defined as

$$m(a/t, \theta/\pi) = 1 - (a/t)^2(\theta/\pi)^{0.2}, \tag{52}$$

$$\frac{\partial m(a/t, \theta/\pi)}{\partial(a/t)} = -2(a/t)(\theta/\pi)^{0.2}, \tag{53}$$

which are empirical functions developed by Kurihara et al. (1988). When the exponents in the equation for $m(a/t, \theta/\pi)$ are chosen to be 2 and 0.2 (see Equation 52), the predicted net-section-collapse moments of pipes with both short and long deep flaws compare reasonably well with the experimental data (Kurihara et al., 1988). When these exponents are assigned large positive values, m approaches 1 and the resulting Kurihara modifications to the net-section-collapse equations degenerate to the original equations. In that case, the difference

Table 1. Geometric parameters and material properties for pipe fracture analysis

Parameters	Example set 1	Example set 2	Example set 3
	Geometry:		
$D_0^{(a)}$, mm (inches)	404.2 (15.91)	554.7 (21.84)	170.5 (6.71)
t, mm (inches)	26.4 (1.04)	26.4 (1.04)	7.75 (0.305)
θ/π	$\frac{1}{16}, \frac{1}{4}$	$\frac{1}{4}$	$\frac{1}{4}$
a/t	$\frac{1}{2}$	$\frac{1}{2}$	$\frac{1}{2}$
	Material Properties:$^{(b)}$		
σ_0, MPa (ksi)	241 (35)	241 (35)	345 (50)
E, GPa (ksi)	207 (30,000)	206 (29,900)	207 (30,000)
ν	0.29	0.29	0.3
α	1	1	1
n	3, 10	2, 5, 10	2

(a) $D_0 =$ outer diameter of the pipe.
(b) The stress-strain ($\sigma - \varepsilon$) curve is represented by: $\varepsilon/\varepsilon_0 = \sigma/\sigma_0 + \alpha(\sigma/\sigma_0)^n, \varepsilon_0 = \sigma_0/E$.

between the SC.ENG1 and SC.ENG2 methods also vanishes. In this study, however, the exponents suggested by Kurihara et al. (i.e., 2 and 0.2) were used for the development of SC.ENG2 method. Further studies are needed to determine if the same exponents apply for shallow cracks.

Equations 4 and 26 provide closed-form expressions of J_e and J_p, respectively. This makes the proposed estimation methods computationally feasible and attractive for the development of probabilistic fracture-mechanics models. See Rahman (1996, 1997) for further details on probabilistic analyses based on the SC.ENG2 method developed here.

6. Numerical examples

In this section, several numerical examples are presented to illustrate the SC.ENG1 and the SC.ENG2 methods for predicting J-integral at the deepest point of the surface crack subjected to pure bending load. In all cases, elastic–plastic finite-element results were used to evaluate the accuracy of the proposed methods. Three example sets were considered. In Example Set 1, the finite-element results were produced from a parallel study by the authors (Krishnaswamy et al., 1995). Krishnaswamy (1995) has details of finite element modeling of surface cracks by shell/line spring elements and three-dimensional solid elements. The results of mesh refinement and validation of line-spring model by three-dimensional solid model are also available in Krishnaswamy (1995). They will not be repeated here. In Example Sets 2 and 3, the finite-element solutions developed by researchers other than the authors were used to verify the J-estimation results. The input parameters describing pipe geometry, crack size, and material properties in these examples are defined in Table 1. The Ramberg–Osgood model (Equation 12) was used for the material stress-strain curve.

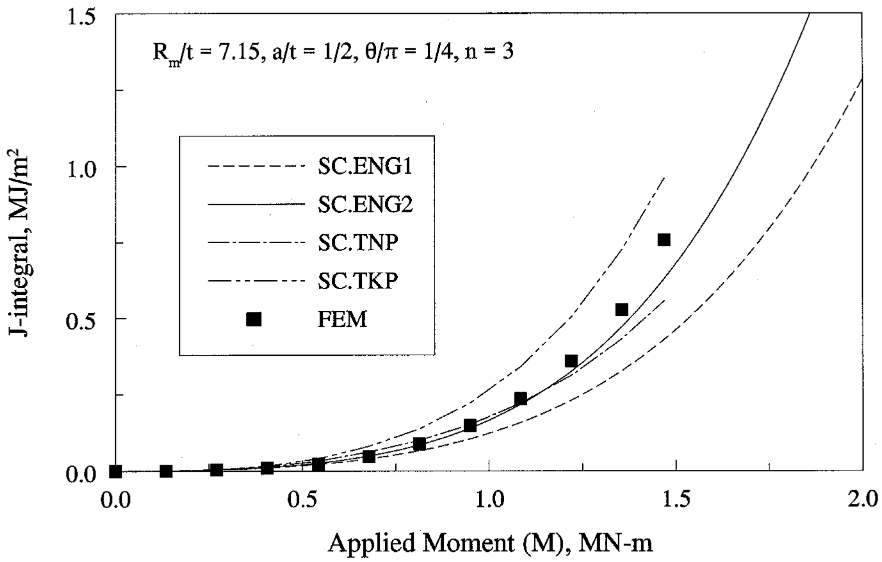

Figure 3. Comparisons of J-integral by various estimation methods with the finite-element results for surface-cracked pipes under pure bending when $\theta/\pi = 1/4$ and $n = 3$.

6.1. Example set 1

In Example Set 1, a medium-size pipe with an outer diameter of 404.2 mm (13.91 inches) which is subjected to pure bending was analyzed. The finite element results were generated by the ABAQUS computer program (ABAQUS, 1993) and using the line-spring/shell elements. The results from the line-spring/shell model were previously validated against those from the full-scale three-dimensional solid model (Krishnaswamy, 1995). Hence, the line-spring FEM results should be adequate in validating the J-estimation results. As shown in Table 1, four pipe cases, involving two different crack lengths (e.g., $\theta/\pi = \frac{1}{16}$ and $\frac{1}{4}$) and two different hardening exponents (e.g., $n = 3$ and 10), were considered. In all cases, the crack depth was fixed to be 50 percent of the wall thickness.

Figures 3 through 6 show the plots of J versus M obtained by the SC.ENG1 and SC.ENG2 methods and the elastic–plastic FEM. The comparisons with the FEM results suggest that the SC.ENG2 method provides reasonably accurate estimates of J-integral for various applied loads for various combinations of crack length (θ/π) and material constant (n). The agreement between the SC.ENG2 and FEM solutions is excellent when θ/π or n is larger. Figures 3 through 6 also show the corresponding results from the SC.ENG1 method which predicted smaller J compared with both SC.ENG2 and finite-element solutions. Since, the Kurihara modification in SC.ENG2 method lowers the net-section-collapse moment from the original equations, the equivalent thickness, t_e is larger in SC.ENG1 method than that in SC.ENG2 method. Therefore, in the SC.ENG1 method, the values of $H(a/t)$ and $\mathrm{d}H(a/t)/\mathrm{d}(a/t)$ functions (Note: $H(a/t) = t/t_e$) would be smaller resulting smaller J_p by the SC.ENG1 method as compared with that by the SC.ENG2 method (see Equation 26). Hence, the trend shown in these figures is expected.

Figures 3 through 6 also show the results from the existing J-estimation methods, such as the SC.TNP and SC.TKP methods, for the same pipe cases. The results by these methods were produced to facilitate comparisons with the SC.ENG1 and SC.ENG2 methods and

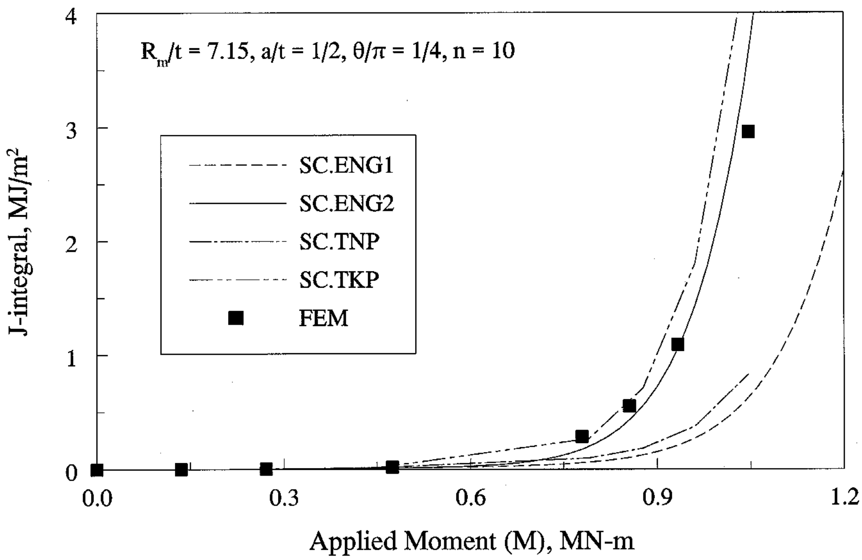

Figure 4. Comparisons of J-integral by various estimation methods with the finite-element results for surface-cracked pipes under pure bending when $\theta/\pi = 1/4$ and $n = 10$.

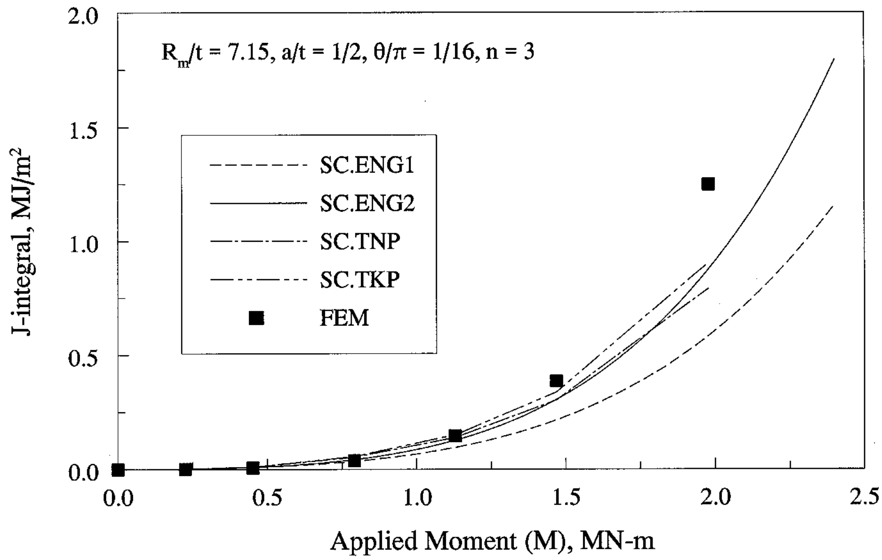

Figure 5. Comparisons of J-integral by various estimation methods with the finite-element results for surface-cracked pipes under pure bending when $\theta/\pi = 1/16$ and $n = 3$.

hence, to determine the level of technical improvements by this newly developed estimation methods. From the above figures, it appears that the SC.ENG2 method provides more accurate solutions of J-integral than either the SC.TNP or the SC.TKP methods for all of the pipe cases considered in this study. However, more numerical studies with various pipe geometry (R_m/t ratio) and crack size parameters (a/t and θ/π ratios) need to be undertaken to make a generic conclusion.

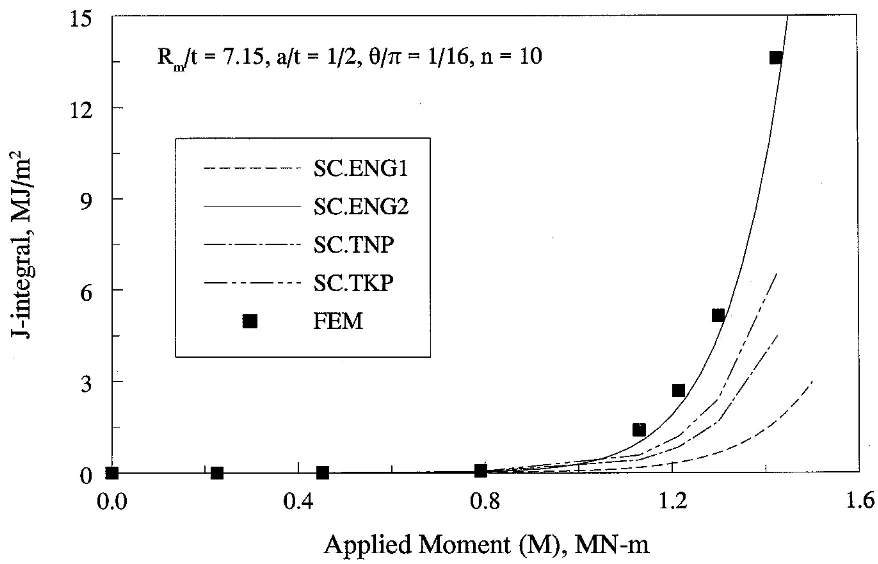

Figure 6. Comparisons of J-integral by various estimation methods with the finite-element results for surface-cracked pipes under pure bending when $\theta/\pi = 1/16$ and $n = 10$.

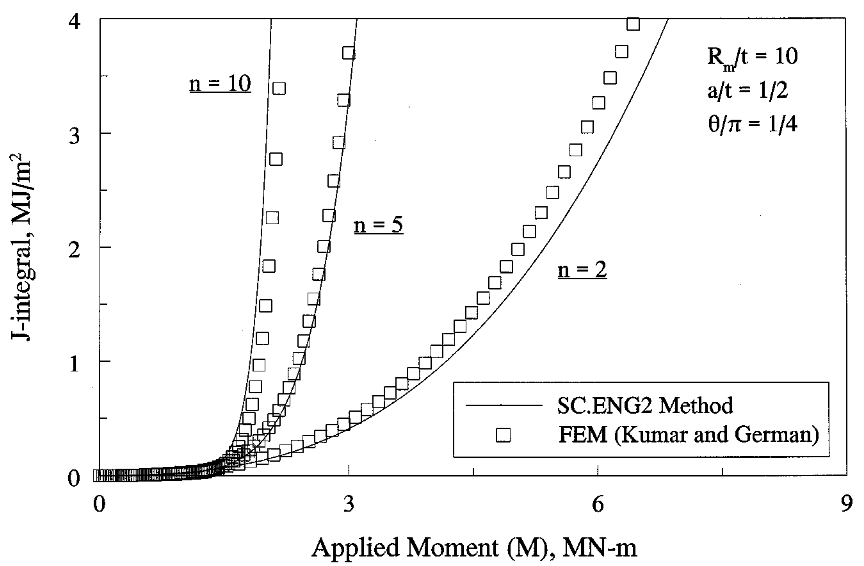

Figure 7. Comparisons of J-integral by the SC.ENG2 method with the finite-element results of Kumar and German (1988) for surface-cracked pipes under pure bending.

6.2. EXAMPLE SET 2

In Example Set 2, a large 554.7-mm (21.84-inch) diameter (outer) pipe under pure bending was analyzed. The finite element solutions were developed by Kumar and German (1988) using the line-spring/shell elements and the ADINA computer code (ADINA, 1981). Three values of material hardening exponent, $n = 2, 5$, and 10 were chosen to determine the sensitivity of J. Other input details are given in Table 1.

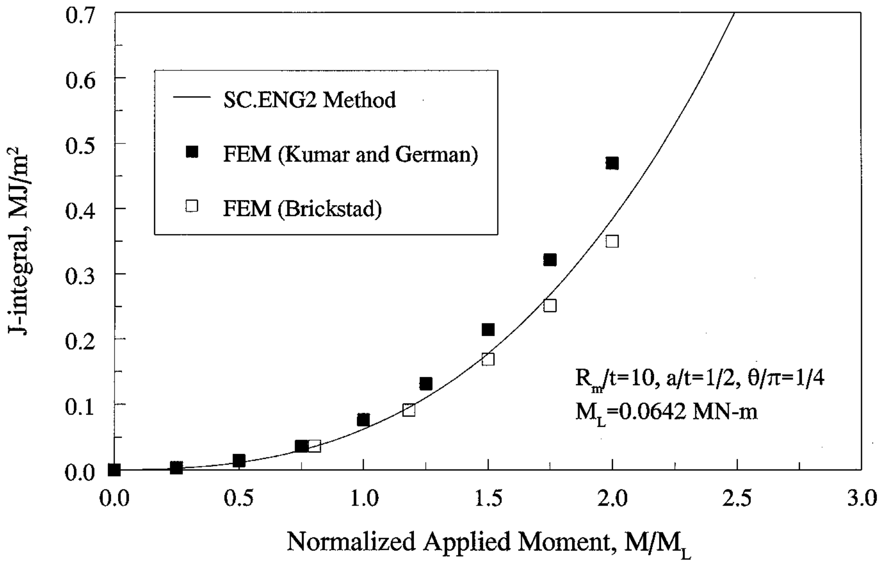

Figure 8. Comparisons of J-integral by the SC.ENG2 method with the finite-element results of Brickstad (1992) and Kumar and German (1988) for surface-cracked pipes under pure bending.

Figure 7 shows the plots of J versus M obtained by the SC.ENG2 method and the finite element analysis by Kumar and German (1988). The comparisons with FEM results suggest that the SC.ENG2 method provides accurate estimates of J for all three values of n. The agreement between SC.ENG2 and FEM solutions is excellent when n is greater. Similar observation was also made in the comparisons of results using authors' own FEM solutions.

6.3. Example set 3

In Example Set 3, a small-size pipe with an outer diameter of 170.5 mm (6.71 inches) also under pure bending was analyzed by Brickstad (1992) using the ABAQUS computer program (ABAQUS, 1993). For this example, elastic–plastic finite element results were also available from the previous work of Kumar and German (1988) using the ADINA computer program (ADINA, 1981). In both work, line-spring/shell models were used for the finite element simulation. Table 1 gives the input parameters for this pipe.

The FEM results of J-integral from Brickstad (1992) are shown in Figure 8 as a function of applied load. In this figure, the horizontal co-ordinate represents the applied bending moment normalized with respect to the limit-moment of the uncracked pipe. Two sets of finite-element results are presented and they correspond to the solutions by Brickstad (open points) and Kumar and German (closed points). The ABAQUS solutions by Brickstad involved 8-noded shell elements and 3-noded nonlinear line spring elements. The ADINA solutions by Kumar and German involved influence functions which were developed using also the shell and line spring elements. The J-integral values by the Kumar and German analysis are slightly higher than those by Brickstad. Also, plotted in the same figure are the results of the SC.ENG2 method. The comparisons with the FEM results suggest that the SC.ENG2 method can provide very accurate predictions of J for various applied moments. For this particular example, the SC.ENG2 results appear to be closer to Brickstad's ABAQUS solutions.

7. Summary and conclusions

Two new methods, known as SC.ENG1 and SC.ENG2, were developed to estimate the energy release rates of circumferentially surface-cracked pipes with finite-length internal flaws subject to remote bending loads. They are based on the deformation theory of plasticity, constitutive law characterized by Ramberg–Osgood model, and an equivalence criterion incorporating reduced thickness analogy for simulating system compliance due to the presence of a crack. For the equivalence criterion, the SC.ENG1 and SC.ENG2 methods are based on the use of original net-section-collapse equations and Kurihara-modified net-section-collapse equations, respectively. In either method, closed-form solutions were developed in terms of elementary functions for an approximate evaluation of J-integral. The methods are general and can be applied in the complete range between the elastic and fully plastic conditions.

Several numerical examples are presented to illustrate the proposed methods. To evaluate their accuracy, J-integral solutions for several pipe diameters, crack sizes, and material constants were obtained from a number of elastic–plastic finite-element analyses. The comparisons of results predicted by the new methods with those from the finite element method showed that for a given applied moment the SC.ENG1 method would underpredict J, while the SC.ENG2 method would provide very good predictions of the energy release rates. It appears that the SC.ENG2 method, which uses the Kurihara modifications to net-section-collapse equations, is superior to the SC.ENG1 method, which uses the original net-section-collapse equations. However, further studies are needed to validate the SC.ENG2 method by varying pipe geometry and crack-size parameters.

The comparisons of results from the existing estimation methods showed that the SC.ENG2 method provides more accurate estimates of J-integral than either the SC.TNP or the SC.TKP methods for the pipe cases considered in this study. However, more numerical studies are needed to support this conclusion.

Acknowledgments

The authors would like to thank Mr. Michael Mayfield and the U.S. NRC Office of Research, Electrical, Materials, and Mechanical Engineering Branch for their encouragement and support of this effort as part of the U.S. NRC's 'Short Cracks in Piping and Piping Welds' Program, Contract No. NRC-04-90-069. Their support and guidance are sincerely appreciated. The first author would also like to thank Drs. G. Wilkowski and P. Krishnaswamy for their valuable comments and Dr. R. Mohan for conducting a few finite element analyses.

Appendix A. The function $\mathrm{I}_B(a/t, \theta/\pi)$

According to the definition

$$\begin{aligned}\mathrm{I}_B(a/t,\theta/\pi) &= 2\theta(R_m - t/2)\int aF_B^2(a/t,\theta/\pi)\,\mathrm{d}a + 2\theta\int a^2F_B^2(a/t,\theta/\pi)\,\mathrm{d}a \\ &= 2\theta(R_m - t/2)\,\mathrm{I}_{B_1}(a/t,\theta/\pi) + 2\theta\,\mathrm{I}_{B_2}(a/t,\theta/\pi),\end{aligned} \tag{54}$$

where,

$$\mathrm{I}_{B_1}(a/t,\theta/\pi) = \int aF_B^2(a/t,\theta/\pi)\,\mathrm{d}a \tag{55}$$

and

$$\mathrm{I}_{B_2}(a/t,\theta/\pi) = \int a^2 F_B^2(a/t,\theta/\pi)\,\mathrm{d}a. \tag{56}$$

Using $F_B(a/t,\theta/\pi)$ from Equation 6, the expressions of $\mathrm{I}_{B_1}(a/t,\theta/\pi)$ and $\mathrm{I}_{B_2}(a/t,\theta/\pi)$ can be further reduced to

$$\begin{aligned}\mathrm{I}_{B_1}(a/t,\theta/\pi) \;=\; & t^2[0.605(a/t)^2 - 0.07309(a/t)^3 + 3.08909(\theta/\pi)^{0.565}(a/t)^{3.565}\\ & +\{0.002484 - 1.5581(\theta/t)\}(a/t)^4 - 0.21859(\theta/\pi)^{0.565}(a/t)^{4.565}\\ & +0.112944(\theta/t)(a/t)^5 + 4.884412(\theta/\pi)^{1.13}(a/t)^{5.13}\\ & -5.09637(\theta/\pi)^{1.565}(a/t)^{5.565} + 1.33755(\theta/\pi)^2(a/t)^6]\end{aligned} \tag{57}$$

and

$$\begin{aligned}\mathrm{I}_{B_2}(a/t,\theta/\pi) \;=\; & t^3[0.40333(a/t)^3 - 0.05482(a/t)^4 + 2.4124(\theta/\pi)^{0.565}(a/t)^{4.565}\\ & +\{0.001987 - 1.24648(\theta/\pi)\}(a/t)^5 - 0.1793064(\theta/\pi)^{0.565}(a/t)^{5.565}\\ & +0.09412(\theta/\pi)(a/t)^6 + 4.08924(\theta/\pi)^{1.13}(a/t)^{6.13}\\ & -4.32008(\theta/\pi)^{1.565}(a/t)^{6.565} + 1.14697(\theta/\pi)^2(a/t)^7].\end{aligned} \tag{58}$$

Appendix B. Governing differential equations for power-law model

Using the classical beam theory for small deformations, the governing differential equations for a pipe with a pure power law constitutive model (i.e., plastic part only) are as follows (see Figure 2 for the definitions of symbols):

(1) Segment AB ($\hat{a}/2 \leqslant x \leqslant L/2$)

$$\frac{\mathrm{d}^2 y}{\mathrm{d}x^2} = \frac{1}{R_m}\left(\frac{M}{M_k}\right)^n, \tag{59}$$

$$\frac{\mathrm{d}y}{\mathrm{d}x} = \frac{1}{R_m}\left(\frac{M}{M_k}\right)^n x + C_1, \tag{60}$$

$$y = \frac{1}{R_m}\left(\frac{M}{M_k}\right)^n \tfrac{1}{2}x^2 + C_1 x + C_2. \tag{61}$$

(2) Segment BC ($0 \leqslant x \leqslant \hat{a}/2$)

$$\frac{\mathrm{d}^2 y}{\mathrm{d}x^2} = \frac{1}{R_m}\left(\frac{M}{M_k}\right)^n \left(\frac{t}{t_e}\right)^n, \tag{62}$$

$$\frac{\mathrm{d}y}{\mathrm{d}x} = \frac{1}{R_m}\left(\frac{M}{M_k}\right)^n \left(\frac{t}{t_e}\right)^n x + C_3, \tag{63}$$

$$y = \frac{1}{R_m}\left(\frac{M}{M_k}\right)^n \left(\frac{t}{t_e}\right)^n \tfrac{1}{2}x^2 + C_3 x + C_4, \tag{64}$$

where

$$M_k = \frac{4KI\hat{K}}{\pi R_m}, \tag{65}$$

$$K = \frac{\sigma_0}{(\alpha\varepsilon_0)^{1/n}}, \tag{66}$$

and I $\approx \pi R_m^3 t$ is the moment of inertia of an uncracked pipe cross-section. If the remote ends of the pipe in Figure 2 are simply supported (hinged), the appropriate boundary and compatibility conditions can be enforced to determine the constants C_1 to C_4 as

$$C_1 = -\frac{1}{R_m}\left(\frac{M}{M_k}\right)^n \frac{\hat{a}}{2}\left[1-\left(\frac{t}{t_e}\right)^n\right], \tag{67}$$

$$C_2 = \frac{1}{R_m}\left(\frac{M}{M_k}\right)^n \left[-\frac{L^2}{8}+\frac{L\hat{a}}{4}\left\{1-\left(\frac{t}{t_e}\right)^n\right\}\right], \tag{68}$$

$$C_3 = 0, \tag{69}$$

$$C_4 = \frac{1}{R_m}\left(\frac{M}{M_k}\right)^n \left[-\frac{L^2}{8}+\frac{L\hat{a}}{4}\left\{1-\left(\frac{t}{t_e}\right)^n\right\}-\frac{\hat{a}^2}{8}\right]. \tag{70}$$

References

ABAQUS (1993). User's guide and theoretical manual, Version 5.3, Hibbitt, Karlsson and Sorensen, Inc., Pawtucket, RI.

ADINA (1981). User's Manual, Report AE81-1, ADINA Engineering, Watertown, MA.

Ahmad, J., Papaspyropoulos, V., Brust, F.W. and Wilkowski, G.M. (1989). A predictive J-estimation method for circumferentially surface-cracked pipes of power-law hardening materials in pure bending. *Proceedings of the 1989 ASME Pressure Vessels and Piping Conference*, Honolulu, Hawaii, 71–85.

ASME (1992). Boiler and Pressure Vessel Code, Section XI, Appendix H, 1992 Edition.

Brickstad, B. (1992). Numerical analysis of IPIRG cracked pipe experiments subjected to dynamic and cyclic loading, SA/FoU-Report 92/05, Stockholm, Sweden.

Brust, F.W. (1987). Approximate methods for fracture analyses of through-wall cracked pipes, NUREG/CR-4853, U.S. Nuclear Regulatory Commission, Washington, D.C.

Hopper, A., Mayfield, M., Olson, R., Scott, P. and Wilkowski, G. (1995). Overview of the IPIRG-2 program – seismic loaded cracked pipe system experiments. *Transactions of the 13th International Conference on Structural Mechanics in Reactor Technology*.

Hutchinson, J.W. (1968). Singular behavior at the end of a tensile crack in a hardening material. *Journal of Mechanics and the Physics of Solids* **16**, 13–31.

Hutchinson, J.W. (1982). Fundamentals of the phenomenological theory of nonlinear fracture mechanics. *Journal of Applied Mechanics* **49**, 103–197.

Ilyushin, A.A. (1946). The theory of small elastic–plastic deformations. *Prikadnaia Matematika I Mekhanika* **PMM 10**, 347–356.

Kanninen, M.F., Broek, D., Marschall, C.W., Rybicki, E.F., Sampath, S.G., Simonen, F.A. and Wilkowski, G.M. (1976). Mechanical fracture predictions for sensitized stainless steel piping with circumferential cracks, EPRI NP-192, Electric Power Research Institute, Palo Alto, CA.

Krishnaswamy, P., Scott, P., Mohan, R., Rahman, S., Choi, Y.H., Brust, F., Kilinski, T., Francini, R., Ghadiali, N., Marschall, C. and Wilkowski, G. (1995). Fracture behavior of short circumferentially surface-cracked pipe, NUREG/CR-6298, U.S. Nuclear Regulatory Commission, Washington, D. C.

Kumar, V. and German, M.D. (1988). Elastic–plastic fracture analysis of through-wall and surface flaws in cylinders, EPRI NP-5596, Electric Power Research Institute, Palo Alto, CA.

Kurihara, R., Ueda, S. and Sturm, D. (1988). Estimation of ductile unstable fracture of pipe with a circumferential surface crack subjected to bending. *Nuclear Engineering and Design* **106**, 265–273.
Paris, P.C., Tada, H., Zahoor, A. and Ernst, H. (1979). The theory of instability of the tearing mode of elastic–plastic crack growth. *ASTM STP 668, Elastic–Plastic Fracture*, 5–36.
Rahman, S., Brust, F., Nakagaki, M. and Gilles, P. (1991). An approximate method for estimating energy release rates of through-wall cracked pipe weldments. *Fatigue, Fracture, and Risk*, PVP-Vol. 215, San Diego, California.
Rahman, S. and Brust, F. (1992). An estimation method for evaluating energy release rates of circumferential through-wall cracked pipe welds. *Engineering Fracture Mechanics* **43**(3), 417–430.
Rahman, S. and Brust, F. (1992). Elastic–plastic fracture of circumferential through-wall cracked pipe welds subject to bending. *Journal of Pressure Vessel Technology* **114**(4), 410–416.
Rahman, S., Wilkowski, G. and Brust, F. (1996). Fracture analysis of full-scale pipe experiments on stainless steel flux welds. *Nuclear Engineering and Design* **160**, 77–96.
Rahman, S. (1996). Probabilistic elastic–plastic fracture analysis of circumferentially cracked pipes with finite-length surface flaws. *Fatigue and Fracture – 1996 – Volume 1*, PVP-Vol. 323, Montreal, Quebec, Canada.
Rahman, S. (1997). A probabilistic model for elastic–plastic fracture analysis of circumferentially surface-cracked pipes subjected to bending, submitted to the *International Journal of Fracture*.
Rice, J.R. (1968). A path-independent integral and the approximate analysis of strain concentration by notches and cracks. *Journal of Applied Mechanics* **35**, 376–386.
Rice, J.R. and Rosengren, G.F. (1968). Plane strain deformation near a crack-tip in a power-law hardening material. *Journal of Mechanics and the Physics of Solids* **16**, 1–12.
Schmidt, R.A., Wilkowski, G.M. and Mayfield, M. E. (1991). The international piping integrity research group (IPIRG) program: An overview. *Transactions of the 11th International Conference on Structural Mechanics in Reactor Technology, Vol. G2: Fracture Mechanics and Non-Destructive Evaluation – 2*, (Edited by H. Shibata), Tokyo, Japan, Paper No. G23/1, 177–188.
Scott, P. and Ahmad, J. (1987). Experimental and analytical assessment of circumferentially surface-cracked pipes under bending, NUREG/CR-4872, U.S. Nuclear Regulatory Commission, Washington, D.C.
Wilkowski, G.M., Ahmad, J., Barnes, C.R., Brust, F., Ghadiali, N., Guerrieri, D., Jones, D., Kramer, G., Landow, M., Marschall, C.W., Olson, R., Papaspyropoulos, V., Pasupathi, V., Rosenfeld, M., Scott. P. and Vieth, P. (1989). Degraded piping program – Phase II: Summary of technical results and their significance to leak-before-break and in-service flaw acceptance criteria, March 1984–January 1989, NUREG/CR-4082, **8**, U.S. Nuclear Regulatory Commission, Washington, D.C.
Wilkowski, G.M. and others (1991–1994). Short cracks in piping and piping welds program, NUREG/CR-4599, Vols. 1 to 3, Nos. 1 and 2, U.S. Nuclear Regulatory Commission, Washington, D.C.